24th EUROPEAN ROTORCRAFT FORUM
Marseilles, France - 15th-17th September 1998

FM05

Identification Of System Parameters In A Nonlinear Helicopter Model

M. Rohlfs
Deutsches Zentrum für Luft- und Raumfahrt e.V. (DLR)
Institut für Flugmechanik
38108 Braunschweig, Germany

Since regulations for the qualification of helicopter flight simulators were published in the Advisory Circular 120-63 (AC 120-63) of the Federal Aviation Administration (FAA), the need of increasing the simulation fidelity of the helicopter mathematical models becomes more and more relevant to meet the new and more restricted requirements.
In the past the DLR Institute of Flight Mechanics used mainly two approaches to develop helicopter mathematical models. The first one determines coefficients in a linear derivative model using system identification methods. In this case the model is derived from the information which is contained in the used flight test data. The second method is a physical approach where the model is generically derived. Here detailed vehicle characteristics are used to derive the model and flight test data is only needed for the evaluation.
In this paper an advanced integrated approach is introduced. A physically based modular structured nonlinear helicopter model is developed. To improve the overall simulation fidelity, in particular the off-axis responses, parametric extensions are added to the model. The introduced parameters are determined using system identification methods.
The paper shortly describes the helicopter modeling activities at the DLR Institute of Flight Mechanics. The used system identification procedure is explained and the requirements of the AC 120-63 are shortly described. Some comments about the modeled helicopter BO 105 and the used flight test data are made. The helicopter model is discussed in detail and identification and verification results are presented in both, the time and frequency domain.

1 NOTATION

C_D	Drag coefficient
C_{D0}	Drag zero derivative
C_L	Lift coefficient
C_{L0}	Lift zero derivative
$C_{L\alpha}$	Lift α derivative
$C_{\lambda_{0,()}}$	Zero downwash derivative
$C_{\lambda_{c,()}}$	Cos downwash derivative
$C_{\lambda_{s,()}}$	Sin downwash derivative
C_X	Longitudinal force coefficient
$C_{X()}$	Longitudinal force derivatives
C_Y	Lateral force coefficient
$C_{Y()}$	Lateral force derivatives
C_Z	Vertical force coefficient
$C_Z()$	Vertical force derivatives
g	Acceleration due to gravity
$I_{()}$	Moments of inertia
I_{MR}	Main rotor moment of inertia
$k_{()}$	Drag derivatives
$k_{eng,()}$	Engine derivatives
L_{aero}	Aerodynamic roll moment
$L_{inertia}$	Inertial roll moment
m	Mass
$Mach$	Mach number
M_{aero}	Aerodynamic pitch moment

$M_{inertia}$	Inertial pitch moment
N_{aero}	Aerodynamic yaw moment
$N_{inertia}$	Inertial yaw moment
p	Roll rate
Q_{eng}	Engine torque
Q_{rot}	Rotor torque
q	Pitch rate
r	Yaw rate
u	Longitudinal velocity component
v	Lateral velocity component
w	Vertical velocity component
V_r	Rotor tip speed
X_{aero}	Aerodynamic longitudinal force
$X_{inertia}$	Inertial longitudinal force
Y_{aero}	Aerodynamic lateral force
$Y_{inertia}$	Inertial lateral force
Z_{aero}	Aerodynamic vertical force
$Z_{inertia}$	Inertial vertical force
α	Angle of attack
$\beta_{()}$	Blade flapping angle
λ_0	Extended downwash velocity, zero comp.
λ_c	Extended downwash velocity, cos comp.
λ_s	Extended downwash velocity, sin comp.
λ_t	Extended downwash velocity, tail rotor
$\lambda_{0,PP}$	Original downwash velocity, zero comp.
$\lambda_{c,PP}$	Original downwash velocity, cos comp.
$\lambda_{s,PP}$	Original downwash velocity, sin comp.
$\lambda_{t,PP}$	Original downwash velocity, tail rotor
Ω	Rotor angular rate
$\Delta\Omega$	$44.4 - \Omega$
Φ	Roll angle
Θ	Pitch angle
Ψ	Yaw angle
Ψ_R	Rotor azimuth
$\dot{()}$	$d()/dt$
$\ddot{()}$	$d^2()/dt^2$

2 INTRODUCTION

Fig. 1 shows the different helicopter modeling approaches at the DLR Institute of Flight Mechanics.

2.1 System identification approach

The first approach, represented by the left column in Fig. 1, is the classical system identification (SID) procedure. In this approach coefficients in linear derivative models are determined using system identification methods. In this case extensive flight test data is needed for the model determination and validation. The obtained global models are mainly used for the development of control systems [1, 2] and for stability and control analysis. Since the structure of these models is linear, they cover only a small range of the flight envelope, namely the range around the trim condition and they are valid only for small control excitations.

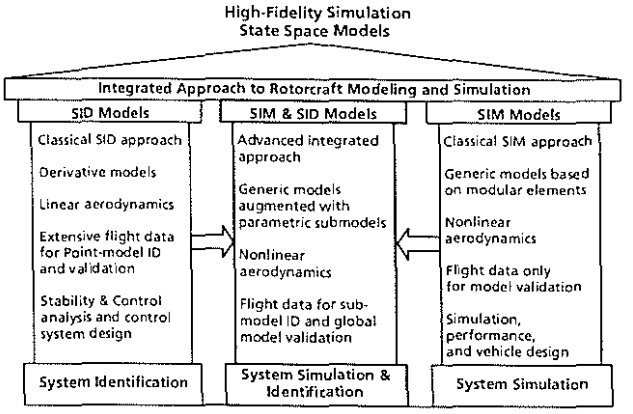

Figure 1: Rotorcraft modeling and validation, the three columns approach

2.2 System simulation approach

The second approach, the classical system simulation (SIM) approach, is represented by the right column in Fig. 1. Here the model is generically derived [3]. The model is modular structured and it is based on detailed vehicle design data. This model is mainly used for real time flight simulation tasks and it is implemented in the institute's helicopter ground based flight simulator. Depending on the model complexity, it can also be used during the design phase for detailed prediction and for overall performance analysis. The main advantages of this model are that it covers the whole flight envelope and that flight test data is only needed to validate the model. The modeling status and fidelity is described in [4].

2.3 Advanced integrated approach

In the DLR Institute of Flight Mechanics a great amount of experience exists in the area of system identification for both, rotary and fixed wing aircraft. One of the latest most challenging tasks was the identification of the model database of the Dornier DO-328 aircraft for a level D flight simulator [5]. Despite the very complex mathematical model and a high number of parameters it turned out, that the system identification methodology is well suited to determine a database which meets the stringent requirements for a level D fixed wing aircraft simulator [6]. In parallel to fixed wing aircraft application, system identification activities also resulted in the determination of accurate linear helicopter models from flight test data [7, 8, 9].

In contrast to fixed wing aircraft models it is not possible to separate a nonlinear helicopter mathematical model in a longitudinal and lateral motion because the helicopter is a highly coupled system. This is mainly due to the rotating blades which have additional degrees of freedom. Therefore it is not possible to identify separated parts of the helicopter model. But first successfull steps [10, 11] showed, that it should be possible to identify system parameters in a nonlinear highly

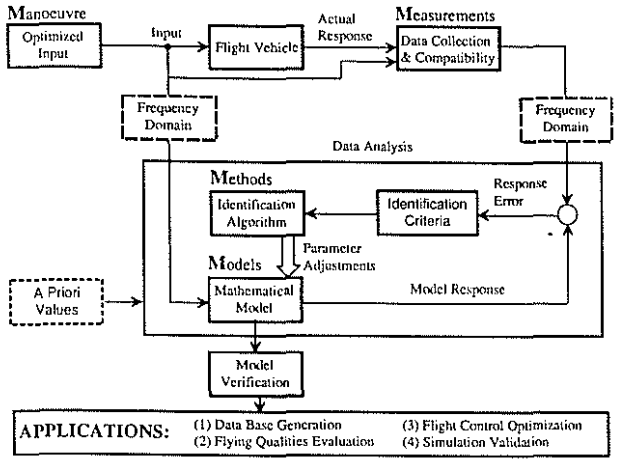

Figure 2: The principle of parameter identification

coupled helicopter simulation model.

In regard of this development it was considered to combine the two helicopter mathematical model development approaches to an integrated system simulation and identification approach. This is represented by the middle column of Fig. 1. The used model is, similar to the model of the 'system simulation approach' generically derived. In addition, parametric extensions are introduced to provide improved descriptions of inaccurately known model components. Flight test data are needed for the determination of the introduced parameters with system identification methods and for the validation of the model.

3 PARAMETER IDENTIFICATION PROCEDURE

Fig. 2 shows the principle of the parameter identification [12]. Specially designed input signals are used to excite the aircraft. Both, control inputs and aircraft response are measured and recorded. The data is checked for compatibility, and errors are corrected as far as possible. The identification techniques can be implemented for working either in the time or frequency domain. Consequently the measured data has the form of time histories or it is transferred into the frequency domain. The aircraft model is formulated as a set of differential equations or respectively as transfer functions. Unknown parameters in the model are adjusted using the differences between measured and computed data to obtain a better agreement. The identification process is usually an iterative process. The adjustment of the parameters is repeated until an accuracy requirement is accomplished or a certain number of iterations is reached.

4 FLIGHT TEST DATABASE

The flight test program was conducted with the BO 105 research helicopter from DLR (Fig. 3). The flight test

Figure 3: BO 105 research helicopter

database consists of tests at different speeds from hover to 110 kts and different input signals like sweep and 3211 signals for all four control inputs. Before using the data for identification and verification, its consistency was checked by performing a flight path reconstruction.

5 NONLINEAR HELICOPTER MODELING

The mathematical model described in this paper is developed for the BO 105 research helicopter from DLR (Fig. 3). The BO 105 is designed as multipurpose light helicopter. Typical use of the highly manoeuverable twin engine vehicle are transport, police and military missions. An important design feature is the hingeless main rotor system. In the following the mathematical modeling of this helicopter is described.

The basic problem of a flight dynamics simulation program is to describe the motion of the vehicle's center of gravity in space. This description is governed by the following system of differential equations.

$$
\begin{aligned}
m\left(\dot{u}+qw-rv\right) &= X_{aero}+X_{inertia} \\
&+ mg\sin\Theta \\
m\left(\dot{v}+ru-pw\right) &= Y_{aero}+Y_{inertia} \\
&- mg\cos\Theta\sin\Phi \\
m\left(\dot{w}+pv-qu\right) &= Z_{aero}+Z_{inertia} \\
&- mg\cos\Theta\cos\Phi \\
I_{xx}\dot{p} - I_{xz}\dot{r}+qr\left(I_{zz}-I_{yy}\right)-I_{xz}pq &= \\
L_{aero}+L_{inertia} & \\
I_{yy}\dot{q} + pr\left(I_{xx}-I_{zz}\right)+I_{xz}\left(p^2-r^2\right) &= \\
M_{aero}+M_{inertia} & \\
I_{zz}\dot{r} - I_{xz}\dot{p}+pq\left(I_{yy}-I_{xx}\right)+I_{xz}qr &= \\
N_{aero}+N_{inertia} & \qquad (1)
\end{aligned}
$$

In a generic approach the right hand sides of these equations are filled up with physically based description of the vehicle with all components contributing to the balance of the three forces and moments. In contrast to a classical 6 degrees of freedom approach for a helicopter simulation program, where only

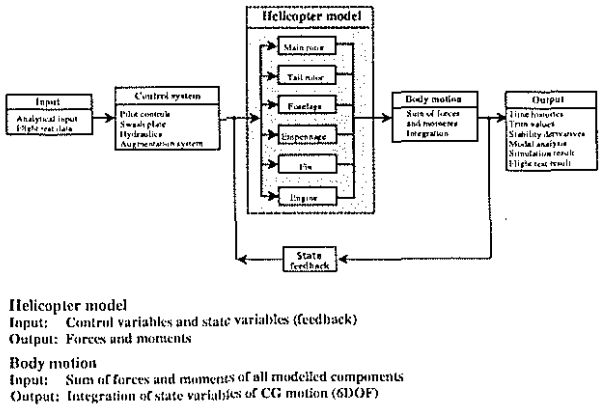

Figure 4: Principle structure of a helicopter simulation program

aerodynamic forces $(X_{aero}, Y_{aero}, Z_{aero})$ and moments $(L_{aero}, M_{aero}, N_{aero})$ are taken into account, the internal inertia forces $(X_{inertia}, Y_{inertia}, Z_{inertia})$ and moments $(L_{inertia}, M_{inertia}, N_{inertia})$ and their internal reactions have to be described in detail.

The most common approach is a modular description where the model of the vehicle is divided up into its components or modules and their individual contributions are added to the right hand side balance of the above system (Eq. 1). For a helicopter these components are

- main rotor including flapping dynamics,
- tail rotor,
- fuselage,
- empennage-horizontal stabilizer,
- fin-vertical stabilizer,
- engine and
- dynamic downwash models for the main and tail rotor.

The principle structure is shown in Fig. 4 as a block diagram.

5.1 Helicopter model modules

In the following the modules are described in more detail.

5.1.1 Main rotor

The standard approach for the main rotor description is the blade element formulation. The rotor is discretisized into the individual blades which are then devided into several segments. The local aerodynamic and inertia forces are then summed up for all segments and all blades to determine the total rotor forces and moments. In addition, the flapping motion of each rotor blade is modeled in a so-called rigid blade formulation where the blade elasticity is neglected.

5.1.2 Tail rotor

The modeling of the tail rotor is the same as for the main rotor. Again the blade element formulation is used to model the aerodynamic and inertia forces of the tail rotor. Due to the high rotational speed of the tail rotor, its flapping motion can be neglected or assumed quasisteady.

5.1.3 Fuselage, empennage, fin

In this model an integrated derivative formulation is made for the helicopter fuselage, empennage and fin.

5.1.4 Engine

The helicopter yaw response, when considered as coupling response, is highly influenced by the dynamic engine and drive train torque. Therefore the basic engine dynamics and the behavior of the rpm governor have to be modeled.

5.1.5 Dynamic downwash

The calculation of the distribution of the induced velocities of the main rotor is based on momentum theory either global or local. The basic description of using trapezoidal downwash distribution in wind axis was given by Glauert as quasisteady description. The extension to a dynamic formulation was developed by Pitt & Peters [13] using the dynamics of thrust and aerodynamic pitch and roll moments produced by the rotor. Their perturbation approach was recently extended to describe the influence of the helicopter motion onto the dynamics of the downwash shape. One of the approaches can be referenced as parametric wake distortion approach. For the downwash of the tail rotor a similar dynamic formulation is used.

5.2 State variables

The mathematical model of the BO 105 described in this paper is of 25^{th} order and has 16 degrees of freedom. The state variables are given in the following list.

- 9 first order differential equations for the rigid body motion $(\dot{u}, \dot{v}, \dot{w}, \dot{p}, \dot{q}, \dot{r}, \dot{\Phi}, \dot{\Theta}, \dot{\Psi})$
- 4 second order differential equations for the blade flapping motion $(\ddot{\beta}_{blue}, \ddot{\beta}_{green}, \ddot{\beta}_{yellow}, \ddot{\beta}_{red})$
- 4 first order differential equations for the dynamic downwash $(\dot{\lambda}_0, \dot{\lambda}_c, \dot{\lambda}_s, \dot{\lambda}_t)$
- 1 second order differential equation for the rotor azimuth $(\ddot{\Psi}_R = \dot{\Omega})$
- 1 second order differential equation for the engine torque $(\ddot{Q}_{eng})$

5.3 Model parts with parameters to be estimated

In the following, the parts of the model where parameters are estimated, are described in more detail.

5.3.1 Blade element aerodynamics

In contrast to most helicopter simulation models the aerodynamic parameters of the rotor and tail rotor blades are not taken from wind tunnel data tables. In this work a derivative approach is made.

$$C_L = C_{L0} + C_{L\alpha}\alpha, \tag{2}$$

$$C_D = C_{D0} + k_1 C_L + k_2 C_L^2. \tag{3}$$

Eq. 2 provides the derivative formulation of the lift coefficient. Eq. 3 describes the modeling of the drag coefficient. All five derivatives, C_{L0}, $C_{L\alpha}$, C_{D0}, k_1 and k_2 can be determined in the identification process. The same aerodynamic formulation is used for the tail rotor. That leads to a total of only ten aerodynamic parameters for both, the main and the tail rotor.

5.3.2 Extended dynamic downwash model

Most of the parameters are used to extend the dynamic downwash model from Pitt and Peters mainly to improve the off axis coupling. The downwash model from Pitt and Peters is described in [13]. Nowadays it is used in most of the efficient helicopter simulation models. A proposal for extending the model is given in [14]. In this paper a more complex approach is made. As an example the extended equation for the cosine downwash is written.

$$\begin{aligned} \dot{\lambda}_c &= \dot{\lambda}_{c,PP} \\ &+ C_{\lambda_c,u}\frac{u}{V_r} + C_{\lambda_c,v}\frac{v}{V_r} + C_{\lambda_c,w}\frac{w}{V_r} \\ &+ C_{\lambda_c,p}\frac{p}{\Omega} + C_{\lambda_c,q}\frac{q}{\Omega} + C_{\lambda_c,r}\frac{r}{\Omega} \\ &+ \dots \end{aligned} \tag{4}$$

Eq. 4 explain the approach. $\dot{\lambda}_{c,PP}$ is the original Pitt and Peters dynamic downwash approach for the cosine part. This approach is then parametrically extended and the derivatives are determined in the estimation process.

5.3.3 Combined fuselage and empennage formulation

For the fuselage and empennage a combined parametric formulation is made.

$$\begin{aligned} C_X &= C_{X0} + C_{X,Mach}Mach \\ C_Y &= C_{Y0} + C_{Y,Mach}Mach \\ C_Z &= C_{Z0} + C_{Z,Mach}Mach \\ C_L &= C_{L0} + C_{L,Mach}Mach \\ C_M &= C_{M0} + C_{M,Mach}Mach \\ C_N &= C_{N0} + C_{N,Mach}Mach \end{aligned} \tag{5}$$

Eq. 5 shows the very simple approach which is made for the forces and moments. The six coefficients are modeled only with the zero and Mach-number dependent derivatives. For the investigated flight test data it was not necessary to introduce other derivatives which for example take the angle of attack or sideslip angle into account.

5.3.4 Engine formulation

The first order differential equation of the rotor speed of rotation is given by:

$$\dot{\Omega} = \dot{r} + \frac{1}{I_{MR}}(Q_{eng} - Q_{rot}) \tag{6}$$

Assuming the engine dynamics due to fuel flow as first order system and the engine governor (fuel flow due to changes in rotor speed of rotation) as PI governor the second order differential equation of the engine torque follows as:

$$\ddot{Q}_{eng} = k_{eng,1}\dot{Q}_{eng} + k_{eng,2}\dot{\Omega} + k_{eng,3}\Delta\Omega \tag{7}$$

6 IDENTIFICATION RESULTS

Twelve runs of flight test data were concatenated. Each run has a duration of 12 seconds. Three velocities, hover, 40 kts and 80 kts were evaluated together. For each velocity all four control inputs, longitudinal, lateral, collective and pedal were used. The input signal for all runs is the DLR 3211-signal. The identification was conducted in the time domain with the NLMLKL program of the Institute of Flight Mechanics. In the following the identification results are presented. First overall results for the velocities, engine states, rates and Euler angles are shown. Then, results which are required to fullfill the criteria given in the AC 120-63 are presented in more detail.

Fig. 5 shows the identification results of the longitudinal, lateral and vertical velocities for all four control inputs, longitudinal, lateral, collective and pedal at all three investigated velocities, hover, 40 kts and 80 kts. The solid line represents the measured data and the dashed line represents the identified results. It can be seen that the overall performance of the identified model is very good. Some discrepancies can be seen. This is possibly due to unknown gust influences, which could not be modeled.

Fig. 6 shows the identification results of the rotor speed of rotation and the engine torque again for all investigated data. In addition the yaw rate is shown. It can be seen, that the engine dynamics are very well modeled although the structure of the model is linear and only three engine parameters are needed (Eq. 7).

Fig. 7 shows the identification results of the roll, pitch and yaw rates for all velocities and all control inputs. Again a very good overall performance of the model can be seen. All cross couplings for all velocities

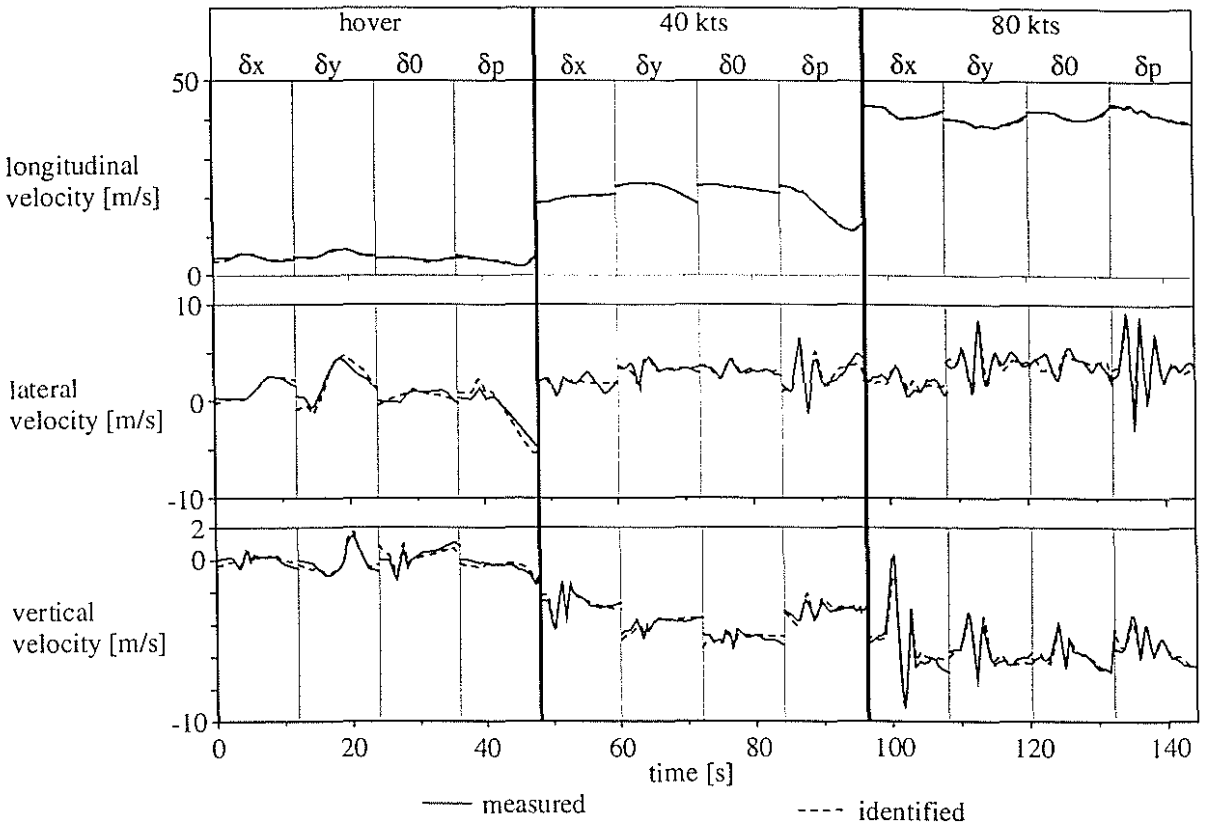

Figure 5: Identification results: velocities

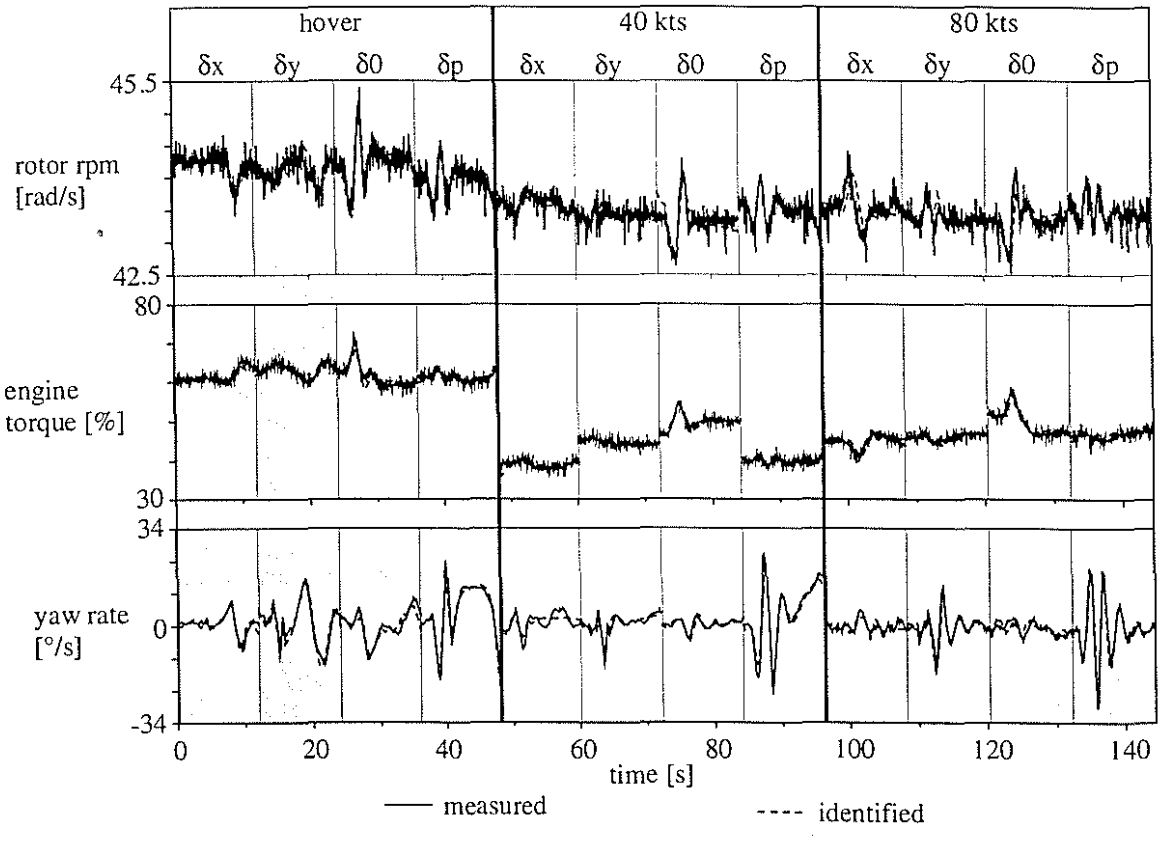

Figure 6: Identification results: engine states

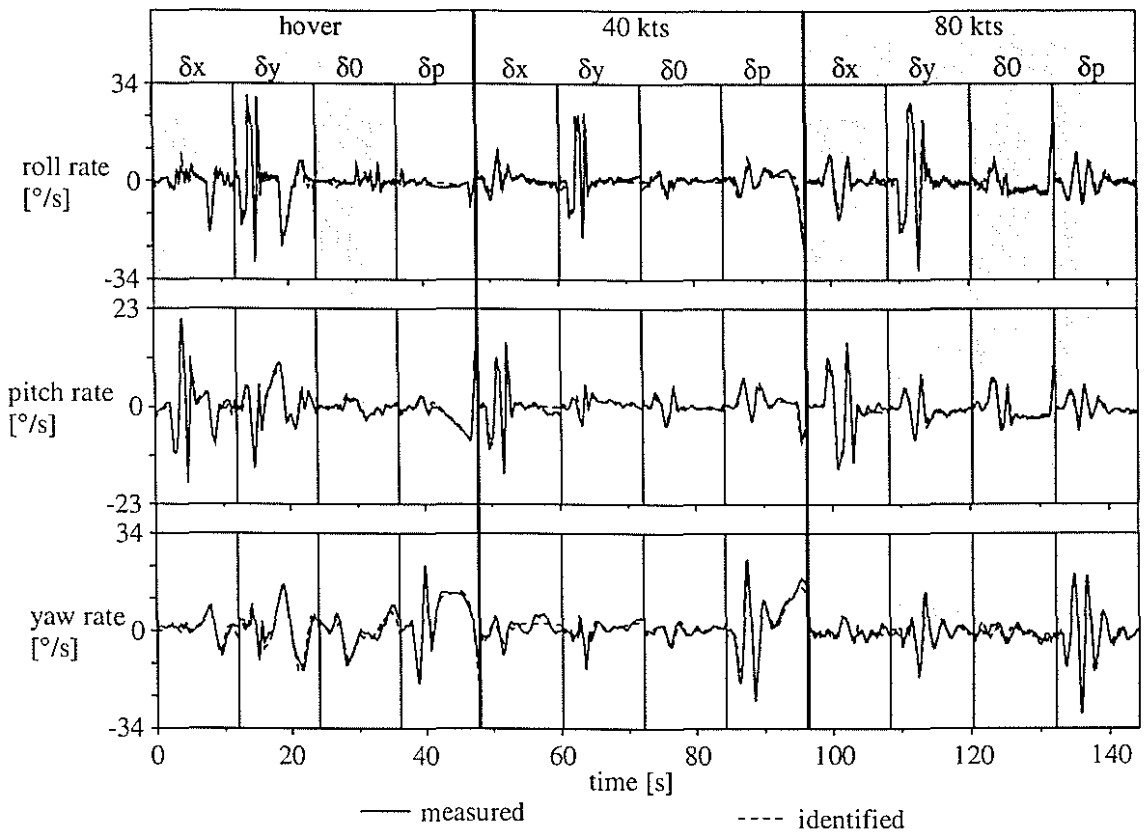

Figure 7: Identification results: rates

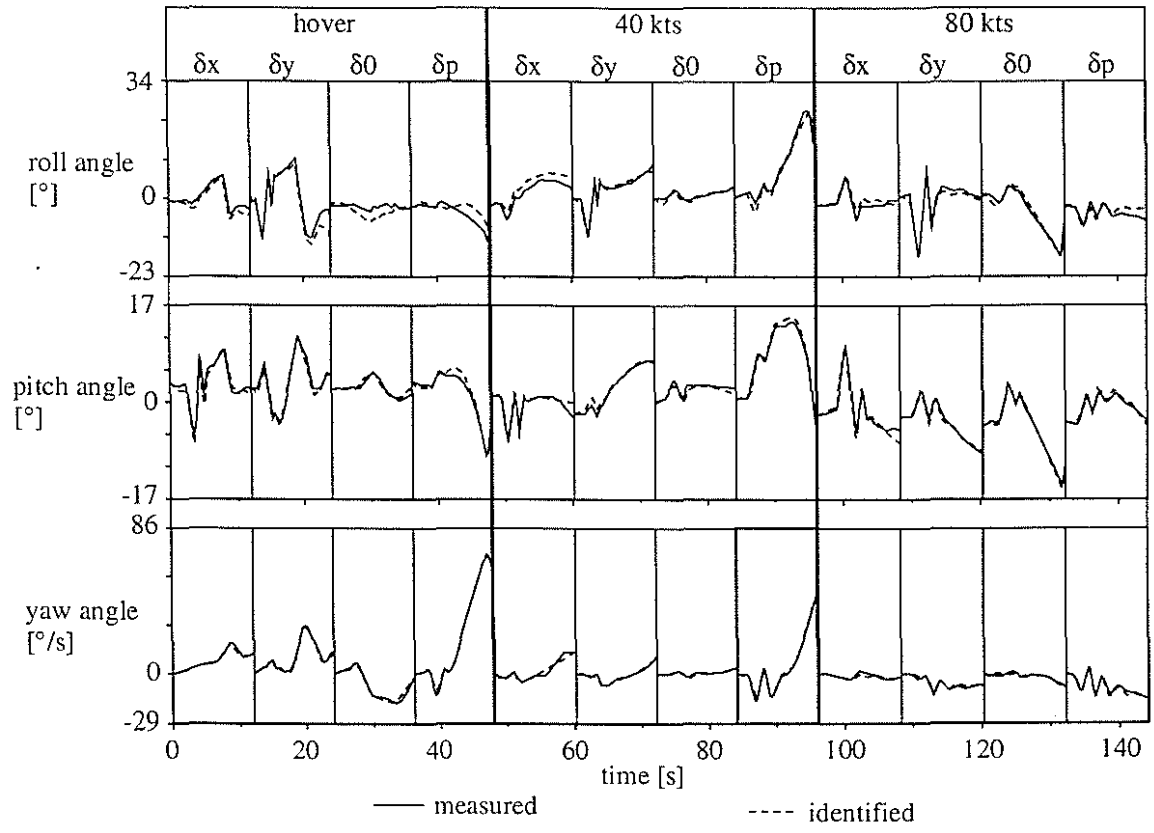

Figure 8: Identification results: Euler angles

and all control inputs are modeled correctly and show the right trend as required in the AC 120-63. Runs for which error boundaries are defined are underlayed white. They will be presented in more detail later.

Fig. 8 shows the identification results of the roll, pitch and yaw angles. Since the rates are well modeled, the fit of attitude angles must be good, too. Some minor discrepancies can be seen which result from the integration of the rates. Small errors in the rates are summed up by the integration and lead to the errors in the attitude angles. Runs for which error boundaries are defined in the AC 120-63 are underlayed white. They will be presented in more detail later.

6.1 Performance with respect to the AC 120-63

In the following the white underlayed runs of Fig. 7 and Fig. 8 for which criteria are given in the AC 120-63 are presented in more detail.

For the presentation of the results, tolerances given in the Advisory Circular AC 120-63 on Helicopter Simulator Qualification [15] of the Federal Aviation Administration (FAA) will be applied. They help to give a quantitative impression about the model accuracy and needs for further improvements. The tolerances are added to the measured flight test data, shown as thin solid line, and the obtained range is plotted as shaded area. The calculated model response is shown as thick solid line which has to stay within the error boundaries to fullfill the AC 120-63 criteria.

The AC 120-63 criteria require step control inputs. Here 3211 signals were used. However, since the 3211 signal consists of five steps, it should be justified to use it instead of the step input signal.

Fig. 9 to Fig. 11 show the direct responses for the hover flight condition. Fig. 9 shows the longitudinal 3211 input signal, the helicopter pitch rate response and the corresponding pitch angle. It can be seen that the pitch rate response is well within the tolerance. The pitch angle fullfills not always the AC 120-63 criteria. Fig. 10 shows the lateral 3211 input signal, the helicopter roll rate response and the corresponding roll angle. Again it can be seen that the rate response is well within the tolerance, whereas the roll angle shows some minor discrepancies. Fig. 11 shows the pedal 3211 input signal, the helicopter yaw rate response and the corresponding yaw angle. It can be seen that the results are similar to the others discussed before.

Fig. 12 to Fig. 14 show the direct responses for the 40 kts flight condition. Again the input signals and corresponding rate responses and attitude angles are shown. The results are similar to the results achieved in hover. The rates and attitude angles are most of the time within the tolerances.

Fig. 15 to Fig. 17 show the direct responses for the 80 kts flight condition. As for the other velocities, the rate and attitude angle results are mostly within the tolerances.

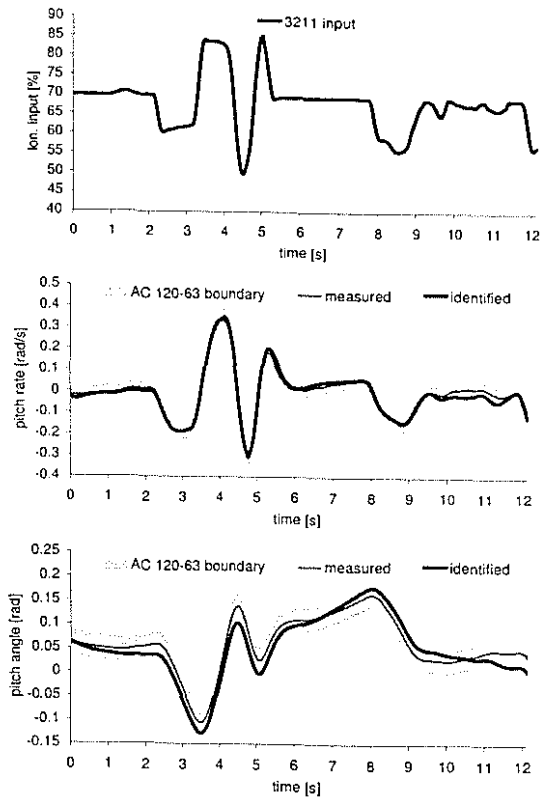

Figure 9: Identification results: direct response due to longitudinal input at hover

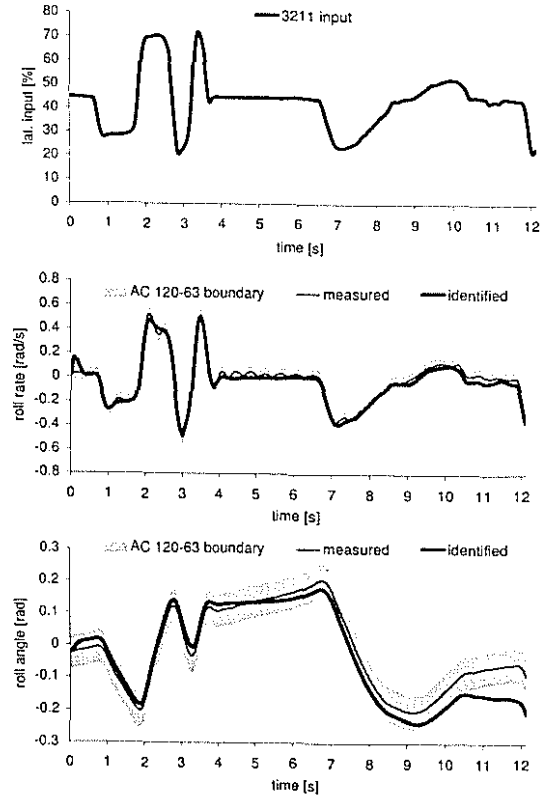

Figure 10: Identification results: direct response due to lateral input at hover

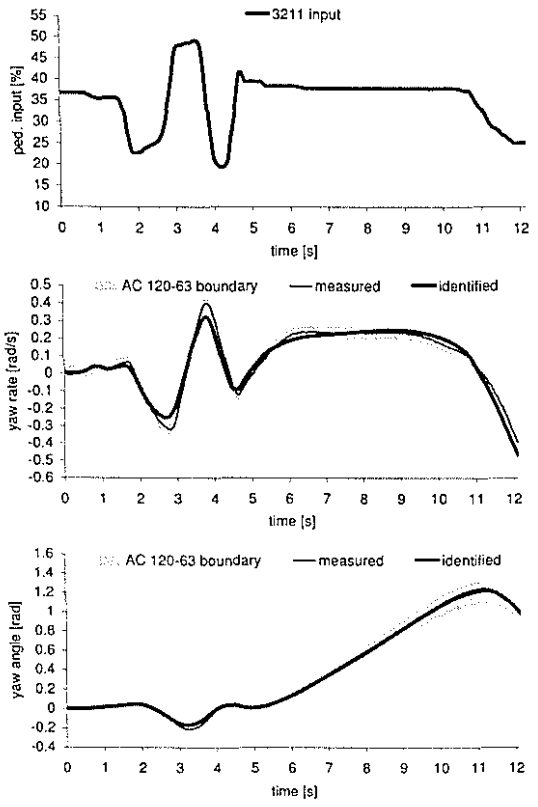

Figure 11: Identification results: direct response due to pedal input at hover

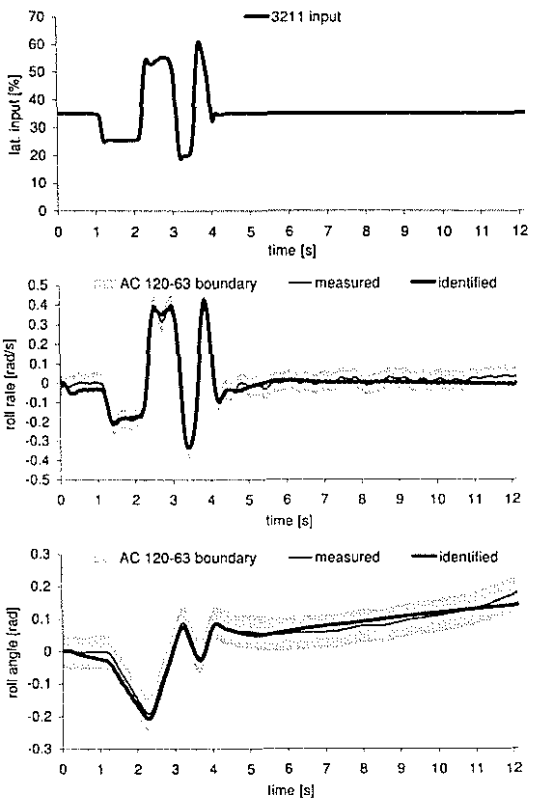

Figure 13: Identification results: direct response due to lateral input at 40 kts

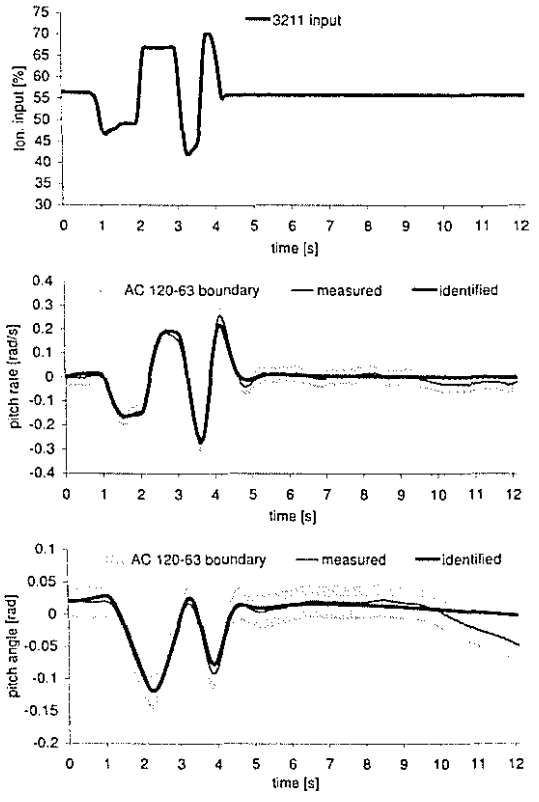

Figure 12: Identification results: direct response due to longitudinal input at 40 kts

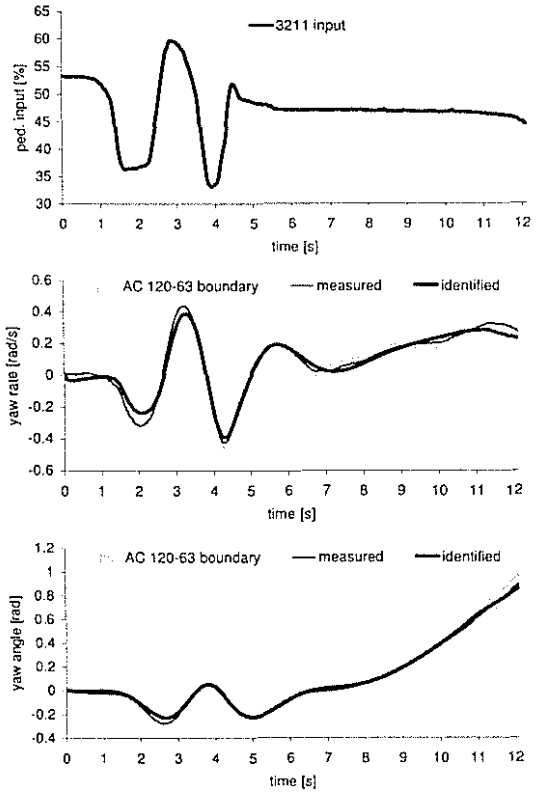

Figure 14: Identification results: direct response due to pedal input at 40 kts

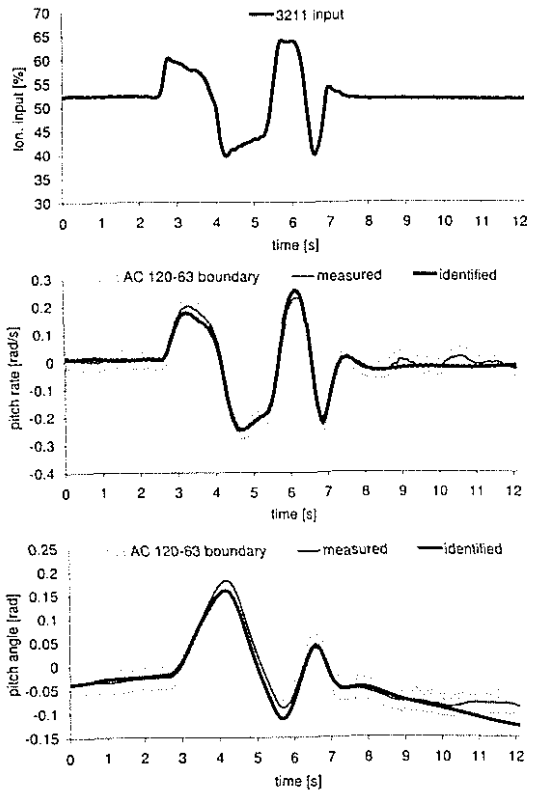

Figure 15: Identification results: direct response due to longitudinal input at 80 kts

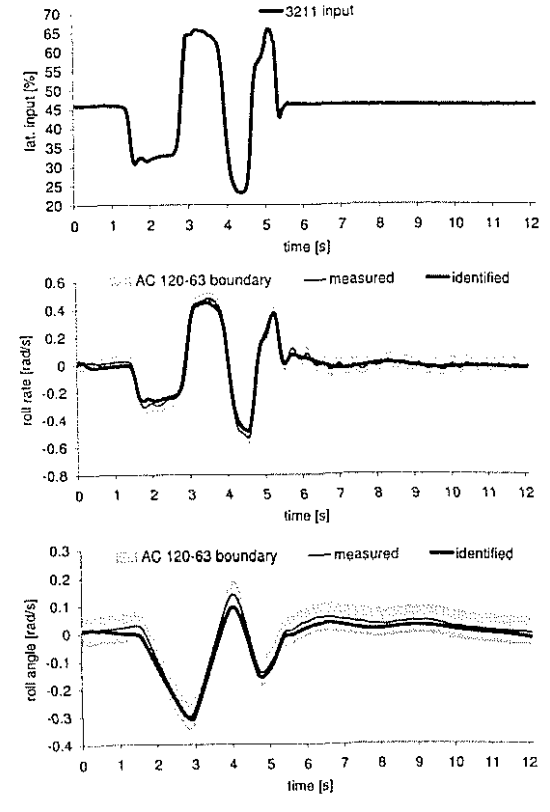

Figure 16: Identification results: direct response due to lateral input at 80 kts

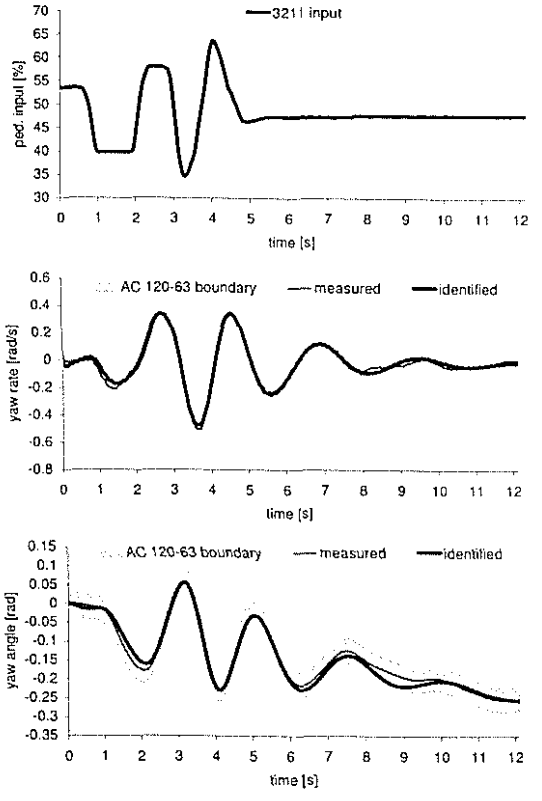

Figure 17: Identification results: direct response due to pedal input at 80 kts

It can be seen that the achieved results not always fullfill the AC 120-63 criteria. This depends mainly on gust influences which could not be taken into account. In addition, data with high amplitudes in the control inputs and consequently high amplitudes in the vehicle response is investigated. 3211 control inputs instead of step control inputs with relative long durations are used. When flight test data with less wind, lower control input amplitudes and shorter duration is investigated, it should be easier to fullfill all AC 120-63 criteria.

7 VERIFICATION RESULTS

To validate the obtained model and to show its prediction capability, a verification simulation was done with data not used in the identification process and with a different input signal. In this case only offsets in the control inputs and initial conditions of the state variables were estimated. Examplary results in the time and frequency domain of the direct responses due to sweep inputs are shown.

7.1 Time domain results

Fig. 18 shows the roll response and the corresponding roll angle due to a sweep input for the hover case as an example. It can be seen that there is a satisfying

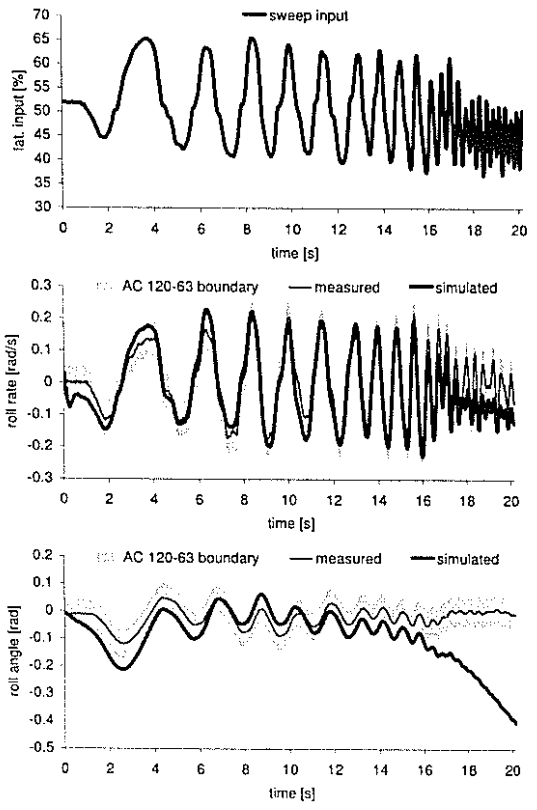

Figure 18: Verification result: direct response due to lateral input at hover

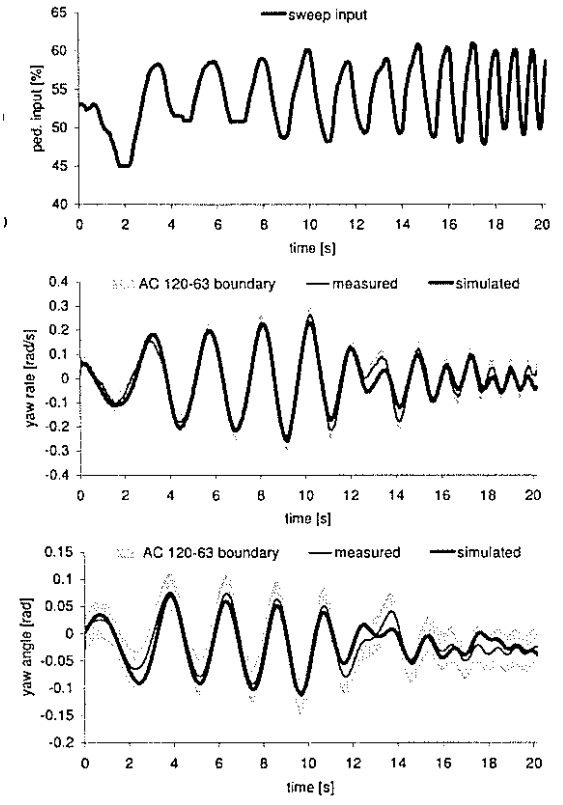

Figure 20: Verification result: direct response due to pedal input at 80 kts

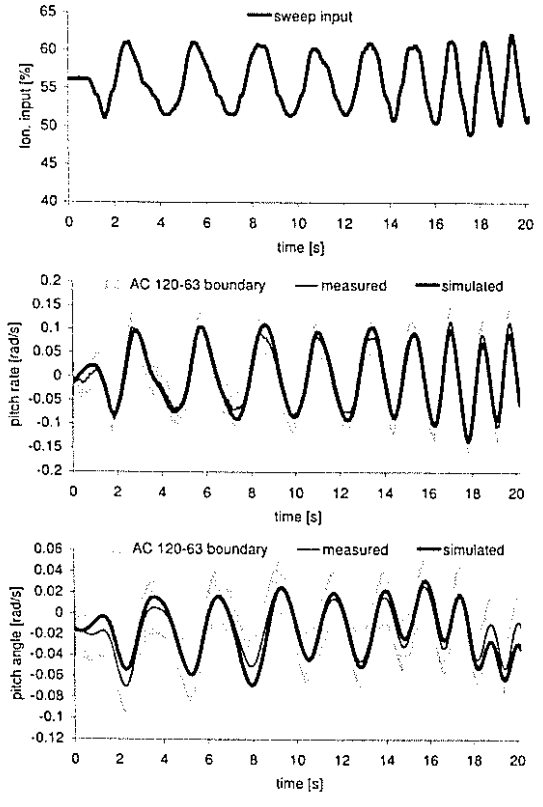

Figure 19: Verification result: direct response due to longitudinal input at 40 kts

match of the roll rate. The match of the roll angle is acceptable although a drift is seen. As example for the 40 kts case Fig. 19 shows the pitch response and pitch angle due to a longitudinal sweep input. In this case the match of the pitch rate and of the pitch angle is very good. For the 80 kts case the results of the yaw rate and yaw angle due to a pedal sweep input are shown in Fig. 20. Again a very good fit between measured data and simulated data is seen for the rate response and for the attitude angle.

7.2 Frequency domain results

In the following the frequency domain results of the above shown sweep responses are presented.

Fig. 21 shows the transfer functions of the measured and simulated roll rate due to the lateral sweep input. It can be seen that there are some deficiencies in the match for higher frequencies. But considering that the data was not used for identification the result is still acceptable.

As a further tool for evaluating the model fidelity, a technique was independently proposed by Hamel [16] and Tischler [9]. In their proposal the relationship between a measured response variable and the corresponding model response is used. When, for example, the measured pitch rate is considered as output and the model pitch rate as input, a 'frequency response' can be calculated. Then, for an ideal model, the mag-

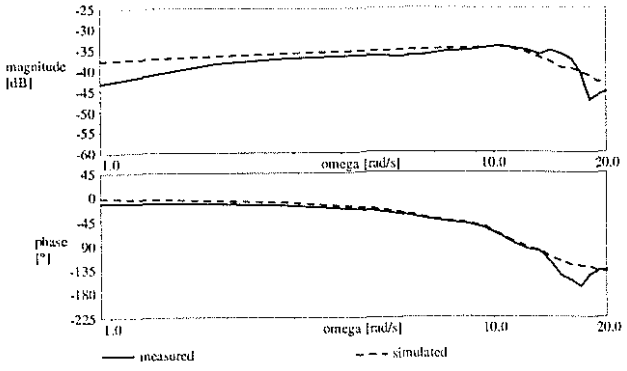

Figure 21: Verification result: transfer functions of measured and simulated roll rate due to lateral input at hover

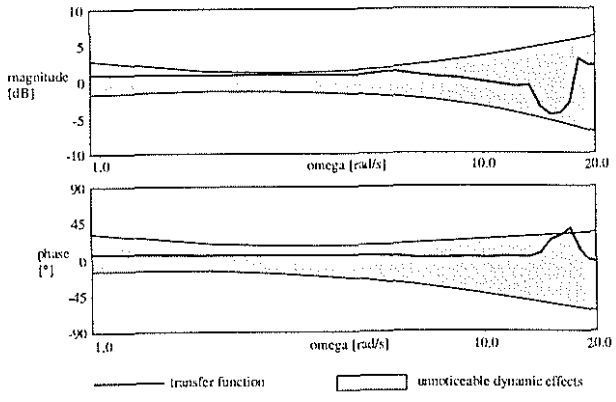

Figure 22: Verification result: transfer function of measured and simulated roll rate at hover, unnoticeable dynamic effects

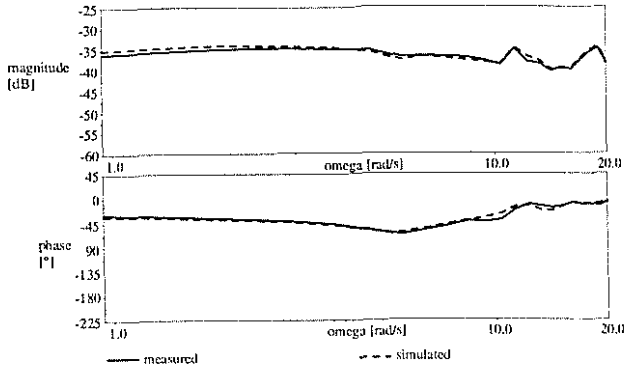

Figure 23: Verification result: transfer function of measured and simulated pitch rate due to longitudinal input at 40 kts

nitude is one and the phase angle is zero. Deviations are caused by differences between model and flight test. Using the frequency domain format, boundaries were used as defined in [17], symbolizing acceptable errors a pilot would not notice in a simulation.

Fig. 22 shows the transfer function of measured and simulated roll rate at hover for a lateral sweep input. It is the same data shown in Fig. 18 which was not used

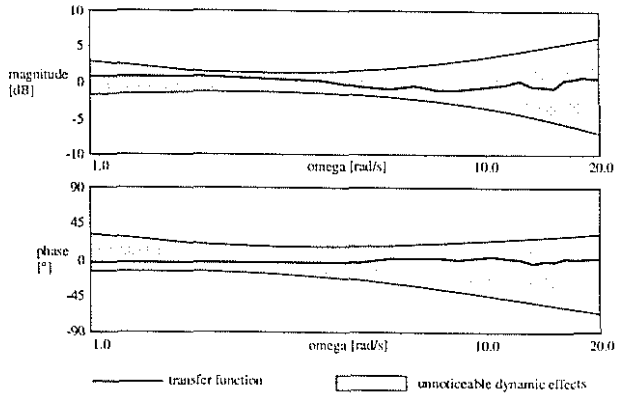

Figure 24: Verification result: transfer function of measured and simulated pitch rate at 40 kts, unnoticeable dynamic effects

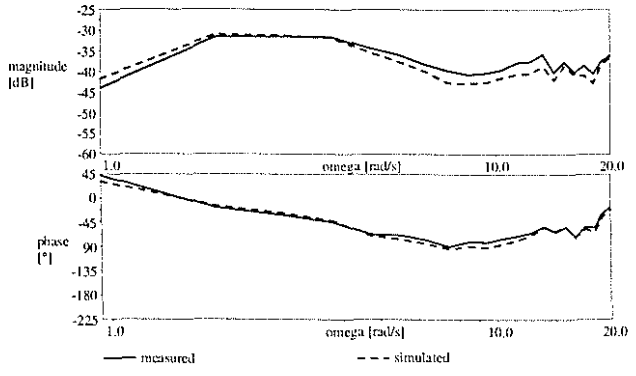

Figure 25: Verification result: transfer function of measured and simulated yaw rate due to pedal input at 80 kts

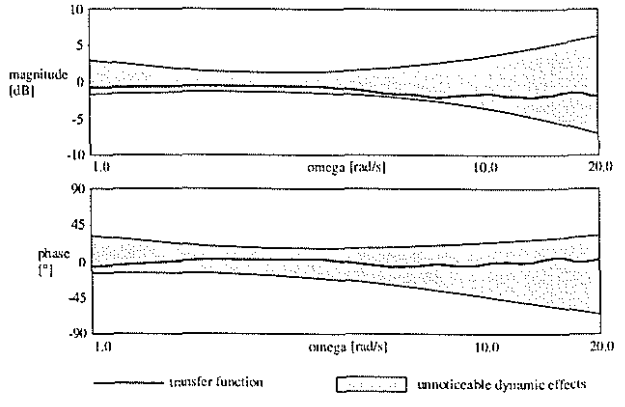

Figure 26: Verification result: transfer function of measured and simulated yaw rate at 80 kts, unnoticeable dynamic effects

for identification. In addition the shaded area of the so-called unnoticeable dynamic effects is shown. It can be seen that the magnitude of the transfer function stays within the boundary. The phase is out of the boundary at higher frequencies. This effect can also be seen in Fig. 21. The match of the transfer functions in this frequency region is not so good, either.

Fig. 23 and Fig. 24 show the results for the 40 kts case corresponding to the results shown in Fig. 20, Fig. 25 and Fig. 26 show the results for the 80 kts case corresponding to the results shown in Fig. 21. It can be seen that the results for higher velocities are better than for the hover case. The match of the transfer functions is good and the results stay always within the area of the unnoticeable dynamic effects.

8 CONCLUSIONS

Based on the experience in the field of helicopter model development and system identification at the DLR Institute of Flight Mechanics, a nonlinear modular structured helicopter model was developed. The goal was to combine the good simulation fidelity of pure identified parametric models with the advantages of generically derived nonlinear model formulations in particular the wide speed range in which the nonlinear model is valid. To improve the overall performance, parametric extensions were introduced to the model. The simulation fidelity of the model was successfully optimized using system identification methods.

The model was extracted from information in flight test data of three different velocities and four different control inputs at each velocity. It was successfully validated with data that was not used in the identification process.

The model shows a very good overall performance at all considered flight tests for the velocities, rates, attitude angles and engine parameters although the criteria given in the Advisory Circular AC 120-63 could not always be fullfilled. The verification simulations show good results, too. Investigations performed in the frequency domain showed that a pilot would not feel a difference between model and real helicopter for the considered verification cases.

It could be shown that the method of parameter identification is well suited to determine parameters in very complex nonlinear and highly coupled dynamic systems.

A great part of flight simulator qualification is the comparison of flight test data with simulated data in the time domain where the simualtion has to stay within certain boundaries. Because of the nature of the parameter identification method, to achieve the best mathematical fit between measured and simulated data, it is best suited to do this work.

References

[1] Kaletka, J., von Grünhagen, W.: *Identification of Mathematical Models for the Design of a Model Following Control System,* American Helicopter Society 45^{th} Annual Forum, May 1989 and Vertica, Vol. 13, No 3, 1989

[2] von Grünhagen, W., Bouwer, G., Pausder, H.-J., Henschel, F., Kaletka, J.: *A High Bandwidth Control System for a Helicopter In Flight Simulator,* International Journal of Control, Vol. 59, No. 1, 1994

[3] von Grünhagen, W.: *Nonlinear Helicopter Model Validation Applied to Realtime Simulations,* The American Helicopter Society Aeromechanics Specialist Conference 1995, Fairfield County, CT, October 1995

[4] Hamers, M., von Grünhagen, W.: *Nonlinear Helicopter Model Validation Applied to Realtime Simulations,* American Helicopter Society 53^{rd} Annual Forum, Virginia Beach, Virginia, April 1997

[5] Jategaonkar, R., Mönnich, W.: *Identification Of DO328 Aerodynamic Database For A Level D Flight Simulator,* AIAA Modeling and Simulation Technologies Conference and Exhibit, New Orleans, LA, 1997

[6] N.N.: *Airplane Flight Simulator Evaluation Handbook,* The Royal Aeronautical Society, London, February 1995

[7] Fu, K.-H., Kaletka, J.: *Frequency-Domain Identification of BO 105 Derivative Models with Rotor Degrees of Freedom,* 16^{th} European Rotorcraft Forum, Glasgow, UK, 1990 and Journal of the American Helicopter Society, Volume 38, No 1, January 1993

[8] Fletcher, J. W.: *Identification of UH-60 Stability Derivative Models in Hover from Flight Test Data,* American Helicopter Society 49^{th} Annual Forum, May 1993

[9] Tischler, M. B.: *System Identification Methods for Aircraft Flight Control Development and Validation,* NASA TM110369, Army TR-95-A-007, October 1995

[10] Rohlfs, M.: *Identification of Nonlinear Derivative Models from BO 105 Flight Test Data,* 22^{nd} European Rotorcraft Forum, Brighton, November 1996

[11] Rohlfs, M., von Grünhagen, W., Kaletka, J.: *Nonlinear Rotorcraft Modeling and Identification,* System Concepts and Integration Panel, 'System Identification for Integrated Aircraft Development and Flight Testing', Paper 23, Madrid, May 1998

[12] Hamel, P. G., Jategaonkar, R. V.: *The Evolution of Flight Vehicle System Identification,* AGARD Stuctures and Materials Panel Specialists' Meeting on ADVANCED AEROELASTIC TESTING AND DATA ANALYSIS, Rotterdam, The Netherlands, May 1995

[13] Pitt D. M., Peters D. A.: *Theoretical prediction of dynamic-inflow derivatives,* Vertica, 1981

[14] Curtiss Jr., H. C., Keller, J. D., Kothmann, B. D.: *On Aerodynamic Modelling for Rotorcraft Flight Dynamics,* 22^{nd} European Rotorcraft Forum, Brighton, November 1996

[15] N.N.: *Advisory Circular AC 120-63,* U.S Department of Transportation, Federal Aviation Administration, October 1994

[16] Hamel, P. G., Kaletka, J.: *Advances in rotorcraft system identification,* AGARD CP 552, 1995

[17] Hodgkinson, J., Wood, J. R.: *Equivalent System Criteria for the Flying Qualities MIL Standard,* in Fuller, S. G., Potts, D. W. Design Criteria for the Future of Flight Controls. Proceedings of the Flight Dynamics Laboratory Flying Qualities and Flight Controls Symposium, 2. - 5. March 1982. Technical Report AFWAL-TR-82-3064

[18] Hamel, P. G. (editor): *Parameter identification,* AGARD LS-104, 1991

[19] Hamel, P. G. (editor): *Rotorcraft system identification,* AGARD AR-280, 1991

[20] Hamel, P. G. (editor): *Rotorcraft system identification,* AGARD LS-178, 1991

[21] Hamel, P. G., Kaletka, J.: *Advances in rotorcraft system identification,* Progress in Aerospace Sciences, Vol.33, 1997

[22] von Grünhagen, W., Bouwer, G., Pausder, H.-J., Henschel, F., Kaletka, J.: *A high bandwith control system for the helicopter in-flight simulator ATTHeS-modelling, performance and applications in Advances in Aircraft Flight Control,* Taylor & Francis, 1996, pp 73-101